

TRUE-AMPLITUDE KIRCHHOFF DEPTH MIGRATION IN ANISOTROPIC MEDIA: THE TRAVELTIME-BASED APPROACH

C. Vanelle and D. Gajewski

email: *claudia.vanelle@zmaw.de*

keywords: *migration, anisotropy, true amplitude, traveltimes*

ABSTRACT

True-amplitude Kirchhoff depth migration is a classical tool in seismic imaging. In addition to a focused structural image it also provides information on the strength of the reflectors in the model, leading to estimates of the shear properties of the subsurface. This information is a key feature not only for reservoir characterisation; it is also important for detecting seismic anisotropy. If anisotropy is present, it needs to be accounted for also during the migration. True-amplitude Kirchhoff depth migration is carried out in terms of a weighted diffraction stack. Expressions for suitable weight functions exist in anisotropic media. However, the conventional means of computing the weights is based on dynamic ray tracing, which has high requirements on the underlying model, in particular if anisotropy must be considered. We suggest a method for the computation of the weight functions that does not require dynamic ray tracing because all necessary quantities are determined from traveltimes alone. In addition, the method leads to considerable savings in computational costs. This so-called traveltimes-based strategy was already introduced for isotropic media. In this work, we extend the strategy to incorporate anisotropy. Examples confirm the image quality and the accuracy of the reconstructed reflectivities.

INTRODUCTION

True-amplitude prestack depth migration can be implemented as a specific form of Kirchhoff migration. In addition to providing a focused structural image of the subsurface, information on the reflection strength at the discontinuities in the medium is also available from such an image. This information can be used for AVO studies, which play a key role in reservoir characterisation.

True-amplitude Kirchhoff depth migration is carried out in terms of a weighted diffraction stack. For each subsurface location, the seismic traces are stacked along the diffraction time surface for that point. Individual weight functions are applied during the stack to recover the reflection amplitude. These weights depend on dynamic wavefield properties. They are usually computed by dynamic ray tracing, together with the diffraction traveltimes.

So far, true-amplitude Kirchhoff depth migration has been almost exclusively applied to PP data under the implicit assumption of isotropy. Since we are dealing with an anisotropic earth, however, the application of isotropic methods leads to problems. Although anisotropy is generally recognised as important in seismic data processing and imaging, it is commonly only considered with respect to kinematic aspects but not to amplitudes. Even the kinematics are in most cases reduced to simple types of media, e.g., media with transverse isotropy.

Anisotropy can have several causes, as for example intrinsic anisotropy or layer-induced anisotropy. Other possibilities are oriented fluid-filled crack systems, and, of course, a combination of these causes, leading to an effective anisotropy. Generally, as soon as there exists an organised structure with a preferred orientation, anisotropy shows if the wavelength of the investigation method is larger than the scale of the structure. This problem of different scales has practical relevance if results from measurements on different scales are to be combined, e.g., surface and bore hole seismics. If anisotropy is not considered, these results will not coincide, i.e., leading to mis-ties etc. (Thomsen, 2002; Juhlin and Windhofer, 1992).

Anisotropic effects are not restricted to kinematics. They have considerable influence on the AVO- or AVA-behaviour of geological interfaces. One example are shales and sands with a similar acoustic impedance. The anisotropy of the shales can lead to a reversal in the polarity of the reflection coefficient that does not occur for isotropy. Another possibility are amplitude changes assigned to the presence of gas if a medium is assumed to be isotropic. In an anisotropic medium, this behaviour can be explained without gas (de Hoop et al., 1999). Therefore, anisotropy must also be acknowledged where amplitudes are concerned.

Several non-Kirchhoff migration techniques for anisotropic media have been suggested. For an overview, see, e.g., Tsvankin et al. (2012). Most of these are, however, restricted to certain symmetries like VTI or TTI media. Sena and Toksöz (1993) and de Hoop and Bleistein (1997) have introduced theoretical representations of Kirchhoff migration in anisotropic media. Their comprehensive and complex theories are, however, not very well suited for an implementation because they require dynamic ray tracing for the generation of the Greens functions. This also applies to a paper on anisotropic true-amplitude migration by Druzhinin (2003). A work by Gerea et al. (2000) gives an anisotropic example for amplitude-preserving migration of multi-component data, but they use a simplified weight function and consider only a horizontally layered VTI medium. Their approach is therefore not applicable to anisotropic media with more complex structure and symmetry.

Even with existing expressions for anisotropic migration weights or Greens functions like those in the works listed above, their computation is not always feasible. One of the purpose of the weights is to countermand the effect of geometrical spreading. Since this is a dynamic wavefield property, true-amplitude migration weight functions are conventionally generated with dynamic ray tracing. These algorithms require smooth models with continuous first and second-order spatial derivatives of the elastic parameters, whereas the output from model-building routines is often blocky. Furthermore, in anisotropic media, ray methods can fail, e.g., in the presence of shear wave singularities.

In order to overcome these demands on the model, Vanelle et al. (2006) have introduced a true-amplitude Kirchhoff migration strategy for isotropic media that employs only kinematic information, i.e., traveltimes, for the generation of the weights. These traveltimes can be computed by kinematic ray tracing, which has lower model requirements, or finite difference eikonal solvers in combination with a perturbation approach (e.g., Ettrich and Gajewski, 1998; Soukina et al., 2003).

Furthermore, the requirements in computer storage are significantly reduced, as the only auxiliary quantity required are the diffraction traveltimes, sampled on coarse grids. A fast and accurate interpolation is then applied to obtain the stacking surfaces on the fine migration grid, where the interpolation coefficients are used for the computation of the weight functions.

In this paper, we suggest the extension of the traveltime-based true-amplitude migration strategy to media with arbitrary anisotropy. The derivation of the weight functions is formally identical to that for the isotropic case. However, in the presence of anisotropy, a different expression for the geometrical spreading must be substituted. A corresponding formulation for geometrical spreading in media with arbitrary anisotropy and heterogeneity was presented by Vanelle and Gajewski (2003), which is a key ingredient for the new anisotropic migration weights.

After the derivation of the anisotropic migration weight function, we provide a brief description of

the traveltimes-based implementation before demonstrating the anisotropic true-amplitude Kirchhoff depth migration with examples for PP and PS reflections¹.

TRUE-AMPLITUDE KIRCHHOFF DEPTH MIGRATION

The displacement $\mathbf{u}(S, G, t)$ that results from an elastic wave generated by a source at the position S and registered by a receiver at R in an arbitrarily anisotropic heterogeneous medium can be expressed by

$$\mathbf{u}(S, G, t) = \sqrt{\frac{\rho(S)V(S)}{\rho(G)V(G)}} \frac{\mathcal{R} \mathcal{G}(S, \gamma_1, \gamma_2)}{\mathcal{L}(G, S)} e^{i\frac{\pi}{2}\kappa} F(t - \tau_R(G, S)) \mathbf{g}(G) \quad (1)$$

(Červený, 2001). In this expression, $\rho(S)$, $\rho(G)$, $V(S)$, and $V(G)$ are the densities and phase velocities at the source and receiver. The quantity \mathcal{R} contains the reflection coefficient and transmission losses. The source signal has the temporal shape given by $F(t)$, and $\tau_R(G, S)$ is the traveltime of the reflected event. The radiation function $\mathcal{G}(S, \gamma_1, \gamma_2)$ at the source depends on the ray parameters γ_1 and γ_2 . The vector $\mathbf{g}(G)$ denotes the polarisation at the receiver. The relative geometrical spreading factor is expressed by $\mathcal{L}(G, S)$, and the factor $e^{i\frac{\pi}{2}\kappa}$ describes phase changes from caustics.

As we wish to reconstruct the reflectivity \mathcal{R} , we stipulate that the migration output $I(M)$ for an imaging point located at M is proportional to \mathcal{R} . According to Schleicher et al. (1993) and Vanelle et al. (2006), $I(M)$ can be obtained from the following integral,

$$I(M) = \frac{-1}{2\pi} \iint d\xi_1 d\xi_2 W(\boldsymbol{\xi}, M) \left. \frac{\partial u(\boldsymbol{\xi}, t)}{\partial t} \right|_{\tau_D(\boldsymbol{\xi}, M)}, \quad (2)$$

where the vector $\boldsymbol{\xi}$ describes the source and receiver positions in the chosen acquisition geometry, e.g., CMP, single shot, or common-offset section. The integral 2 corresponds to a stack along the diffraction traveltimes surface $\tau_D(\boldsymbol{\xi}, M)$, weighted with the function $W(\boldsymbol{\xi}, M)$.

Equation 1 describes the displacement vector, $\mathbf{u}(S, G, t) \equiv \mathbf{u}(\boldsymbol{\xi}, t)$, whereas the diffraction stack 2 uses the magnitude of the displacement, the scalar quantity $u(\boldsymbol{\xi}, t)$. This means that in the case of a three component registration, wave field separation needs to be applied prior to the migration (Dillon et al., 1988).

After a transformation to the frequency domain, the stack integral 2 can be solved in the high frequency limit by applying the method of stationary phase (e.g., Bleistein, 1984). This process is formally identical for isotropic and anisotropic media. However, the geometrical spreading for both types of media is not the same. For anisotropic media, we have according to Schleicher et al. (2001) and Vanelle and Gajewski (2003),

$$\mathcal{L}(G, S) = \frac{1}{V(S)} \left| \frac{\cos \vartheta_s \cos \vartheta_g}{\cos \chi_s \cos \chi_g} \det \mathbf{N}^{-1} \right|^{\frac{1}{2}} e^{-i\frac{\pi}{2}\kappa}, \quad (3)$$

where ϑ_s and ϑ_g are the acute angles between the ray (group) velocity vectors $\mathbf{v}(S)$ and $\mathbf{v}(G)$ at the source and receiver, respectively, and the vertical axis. The angles χ_s and χ_g are made by the respective ray and phase velocities at the source and receiver. In isotropic media, the $\cos \chi_I$ are equal to one because phase and group velocities coincide. Finally, the 2×2 matrix \mathbf{N} contains second-order traveltimes derivatives with respect to the source and receiver coordinates, i.e.,

$$N_{IJ} = - \frac{\partial^2 t(S, G)}{\partial x_s \partial x_g}. \quad (4)$$

Following Schleicher et al. (1993) and substituting the anisotropic geometrical spreading 3, we find that the weight function

$$W(\boldsymbol{\xi}, M) = \sqrt{\frac{\rho(G)}{\rho(S)}} \frac{\sqrt{v_z(G) v_z(S)}}{V(S)} \frac{1}{\mathcal{G}(S, \gamma_1, \gamma_2)} \frac{|\det(\boldsymbol{\Sigma}^T \mathbf{N}_s^r + \boldsymbol{\Gamma}^T \mathbf{N}_g^r)|}{\sqrt{|\det \mathbf{N}_s^r| |\det \mathbf{N}_g^r|}} e^{-i\frac{\pi}{2}(\kappa_s + \kappa_g)}, \quad (5)$$

¹we use the designations PP and PS instead of the mildly cumbersome $qPqP$ and $qPqSV$ although it is well known that in anisotropic media wave propagation generally does not occur in pure modes.

leads to a reconstruction of the reflectivity in arbitrary anisotropic media if it is applied with the stack 2.

In the weight function 5, the configuration matrices Σ and Γ describe the relation between the trace coordinates ξ and the source and receiver positions S and G . Examples can be found in Schleicher et al. (1993). The radiation function at the source can be calculated after Gajewski (1993) or Pšenčík and Teles (1996). The v_z are the vertical components of the ray (group) velocities at the source and receiver. The matrices N_s^r and N_g^r are second-order mixed derivatives of the traveltimes with respect to source/receiver coordinates and the coordinates in the reflector tangent plane at the image point M , i.e.,

$$N_{sIJ}^r = -\frac{\partial^2 t(S, M)}{\partial x_s \partial x_m} \quad \text{and} \quad N_{gIJ}^r = -\frac{\partial^2 t(G, M)}{\partial x_g \partial x_m} . \quad (6)$$

As we do not a priori know the orientation of the reflector surface, it is assumed for each source-receiver combination that it corresponds to the stationary ray. Then the orientation can be obtained from the slowness vectors of the two ray segments at the image point, as described in Vanelle et al. (2006).

Special case: 2.5D

To carry out the stack integral 2, data from a 3D coverage is required. Sometimes, though unfavourable in the presence of anisotropy, data is only available for a single acquisition line. In the special case where the medium is assumed to be invariant in the off-line (i.e. $\xi_2=y$) direction, the so-called 2.5D symmetry (see, e.g., Bleistein, 1986), true-amplitude migration can be carried out by applying a modified stack, which is introduced below. In anisotropic media, this means that wave propagation is restricted to the $\xi_1 - z$ plane, which is the case if the $\xi_1 - z$ plane is a symmetry plane of the anisotropic medium, like TI media or orthorhombic media in a symmetry plane (see, e.g., Ettrich et al., 2001).

Under these conditions, the stack

$$I_{2.5D}(M) = \sqrt{\frac{1}{2\pi}} \int d\xi_1 W_{2.5D}(\xi_1, M) f [u(\xi_1, t + \tau_D(\xi_1, M))] \quad (7)$$

leads to a true-amplitude migrated trace (e.g., Martins et al., 1997). Here, $f[u]$ is a filter operation corresponding to a multiplication of u with $\sqrt{i\omega}$ in the frequency domain (applied instead of the time derivation of u in the 3D case). The 2.5D weight function is simpler than the 3D weight, as $N_{I_{12}}^r = N_{I_{21}}^r = 0$. Introducing $\sigma_I = 1/N_{I_{22}}^r$, the weight function becomes

$$W_{2.5D}(\xi_1, M) = \sqrt{\frac{\rho(G)}{\rho(S)}} \frac{\sqrt{v_z(G) v_z(S)}}{V(S)} \frac{1}{\mathcal{G}(S, \gamma_1, \gamma_2)} \frac{|\Sigma N_s^r + \Gamma N_g^r|}{\sqrt{|N_s^r N_g^r|}} \sqrt{\sigma_s + \sigma_g} e^{-i\frac{\pi}{2}(\kappa_s + \kappa_g)} , \quad (8)$$

where N_I^r is used as abbreviation for $N_{I_{11}}^r$.

In the 2.5D geometry, the orientation of the reflector can also be obtained from the slowness vectors of the two ray segments at the image point, denoted by \mathbf{q}_s and \mathbf{q}_g . We find that

$$N_I^r = N_{I_{xx}} \cos \beta - N_{I_{xz}} \sin \beta , \quad (9)$$

with the mixed second-order traveltime derivatives in the global Cartesian coordinate system,

$$\begin{aligned} N_{s_{xx}} &= -\frac{\partial^2 t(S, M)}{\partial x_s \partial x_m} & N_{s_{xz}} &= -\frac{\partial^2 t(S, M)}{\partial x_s \partial z_m} , \\ N_{g_{xx}} &= -\frac{\partial^2 t(G, M)}{\partial x_g \partial x_m} & N_{g_{xz}} &= -\frac{\partial^2 t(G, M)}{\partial x_g \partial z_m} . \end{aligned} \quad (10)$$

The indices s , g , and m denote the source, receiver, and image point, respectively. The angle β is given by

$$\tan \beta = -\frac{\cos \theta_2 - \cos \theta_1}{\sin \theta_2 - \sin \theta_1} = -\frac{V_g q_{gz} - V_s q_{sz}}{V_g q_{gx} - V_s q_{sx}} , \quad (11)$$

where the V_I are the phase velocities of the ray segments at the image point, and the θ_I are the corresponding phase angles.

The traveltimes-based approach

In this section, we explain how the weight functions 5 and 8 can be computed from traveltimes only. We use the following expression for the traveltimes from a source S at the position \mathbf{s} to a subsurface point M at the position \mathbf{m} (Vanelle and Gajewski, 2002):

$$t^2(\mathbf{s}, \mathbf{m}) = (t_s - \mathbf{p}_s \Delta \mathbf{s} + \mathbf{q}_s \Delta \mathbf{m})^2 - t_s (2 \Delta \mathbf{s} \cdot \mathbf{N}_s \Delta \mathbf{m} - \Delta \mathbf{s} \cdot \mathbf{S}_s \Delta \mathbf{s} + \Delta \mathbf{m} \cdot \mathbf{G}_s \Delta \mathbf{m}). \quad (12)$$

Equation 12 is a hyperbolic expansion of the traveltimes in source and subsurface point coordinates. The traveltimes t_s is that from the source at \mathbf{s}_0 to the subsurface point at \mathbf{m}_0 . We will refer to the combinations of $(\mathbf{s}_0, \mathbf{m}_0)$ as the expansion points that are represented by the coarse grid. The actual source and subsurface point coordinates \mathbf{s} and \mathbf{m} are represented by their respective distances to the expansion point by $\Delta \mathbf{s} = \mathbf{s} - \mathbf{s}_0$ and $\Delta \mathbf{m} = \mathbf{m} - \mathbf{m}_0$. The slowness vectors \mathbf{p}_s and \mathbf{q}_s are the first-order traveltimes derivatives at the source and subsurface point, i.e.,

$$p_{s_i} = -\frac{\partial t}{\partial s_i}, \quad q_{s_i} = \frac{\partial t}{\partial m_i}. \quad (13)$$

Finally, the three matrices

$$S_{s_{ij}} = -\frac{\partial^2 t}{\partial s_i \partial s_j}, \quad G_{s_{ij}} = \frac{\partial^2 t}{\partial m_i \partial m_j}, \quad N_{s_{ij}} = -\frac{\partial^2 t}{\partial s_i \partial m_j} \quad (14)$$

are the second-order derivatives of the traveltimes.

Since the traveltimes are in any event required for the stacking surface, we assume that these are available and sampled on coarse grids. As described in Vanelle and Gajewski (2002), the coefficients in Equation 12 can be determined from the traveltimes tables, with the exception of the vertical slowness at the source. In isotropic media, this coefficient follows immediately from the eikonal equation. In anisotropic media, it can be directly obtained following Červený and Pšenčík (1972) in the 2.5D case, or after Vanelle and Gajewski (2009) for the 3D situation with arbitrary weak anisotropy. Once the slowness vector is known, we can compute the components of the group velocity after Červený and Pšenčík (1972).

For the traveltimes from a receiver G at the position \mathbf{g} to the subsurface point M we use the corresponding expression 12 with \mathbf{g} instead of \mathbf{s} .

The coefficients are then applied for the interpolation of the traveltimes onto the fine migration grid and the weight function. If only first-arrival traveltimes are given, the KMAH indices are zero. If later arrivals are considered, it is convenient to generate the tables for the individual arrivals with an algorithm that outputs them sorted by KMAH, e.g., with the wavefront-oriented ray tracing technique by Coman and Gajewski (2005), and its extension to anisotropic media by Kaschwich and Gajewski (2003).

EXAMPLES

We have applied the method to the simple anisotropic velocity model displayed in Figure 1. In both layers we have chosen $\epsilon = \delta = 0.1$ and $\gamma = 0.1$ corresponding to elliptical symmetry because this symmetry enables us to compute the PP and PS reflectivities analytically (Daley and Hron, 1979) for comparison with the migration results. Ray synthetic seismograms were generated for an explosive source. The required traveltimes tables for the qP - and qSV -waves were computed analytically on grids with a 100 m spacing. The distance between sources was also 100 m. These were the only input data needed for the computation of the true-amplitude weight functions as well as for the interpolation of the diffraction traveltimes onto the migration grid with 10 m spacing in x and z direction.

The depth-migrated PP section is shown in Figure 2a; the PS section in Figure 2b. As we have used the correct elastic parameters for the generation of the traveltimes, the migration result shows the reflector imaged in the correct location.

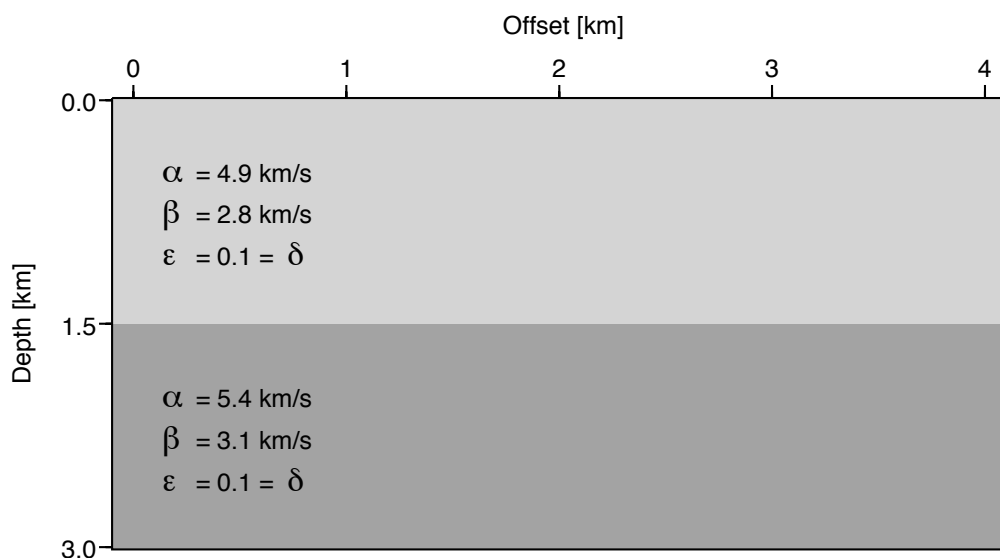


Figure 1: The anisotropic velocity model. Thomsen's parameters were chosen as $\epsilon = \delta = 0.1$ and $\gamma = 0.1$.

Since another aim of the true-amplitude migration is to recover the reflectivity, we have picked the amplitudes from the image gathers. The results are shown together with the analytic solutions in Figure 3a for the PP, and in Figure 3b for the PS reflection. As we can see, both reconstructed AVO curves coincide with the analytic values. The deviations at higher offsets are caused by the limited extent of the receiver line. Due to the asymmetry of the ray paths, the offset range is different for the PP and the PS case.

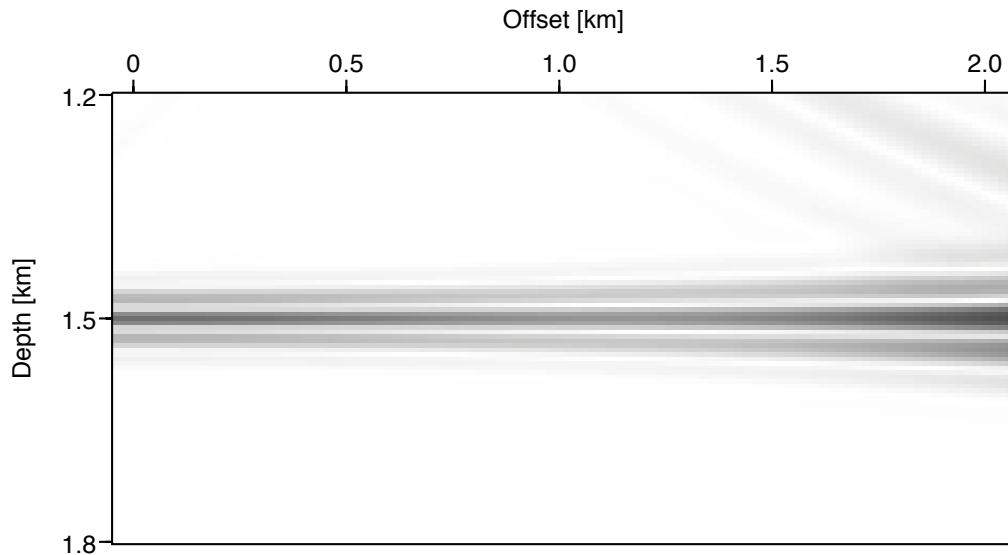
DISCUSSION

Although we have restricted our examples to a simple geometry, we can conclude that our new method is equally suited for complex situations. This conclusion is supported by the complex isotropic synthetic and field data migration examples presented in Vanelle et al. (2006). In that work, we have shown that the structural information as well as the reflectivities are reconstructed with high accuracy by the traveltimes-based method.

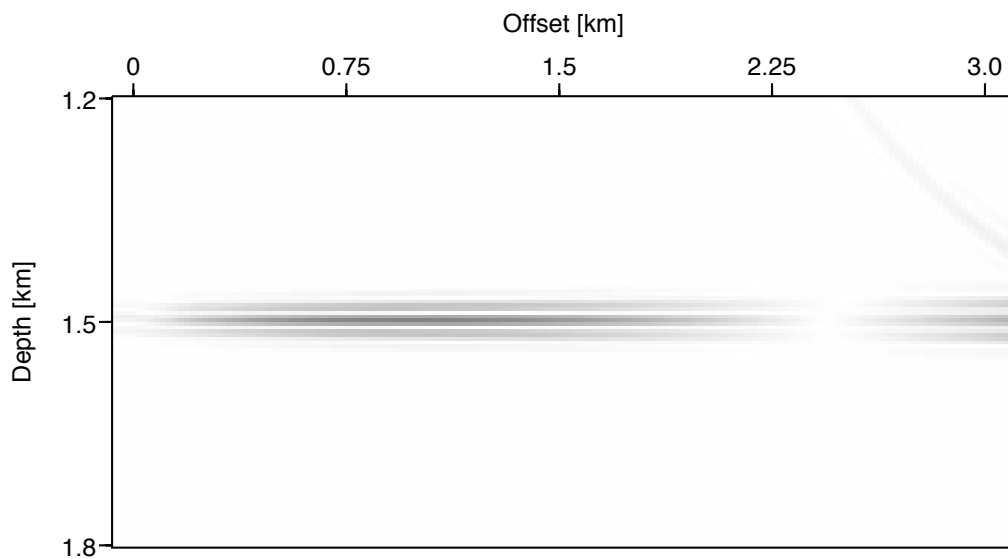
Furthermore, in Vanelle and Gajewski (2003), we have demonstrated the determination of geometrical spreading in heterogeneous anisotropic 3D media, down to examples with triclinic symmetry. Since the coefficients used for the traveltimes interpolation and the anisotropic weight functions suggested here are the same that were used in the spreading determination in Vanelle and Gajewski (2003), our conclusion is justified.

CONCLUSIONS

We have introduced a traveltimes-based strategy for true-amplitude Kirchhoff depth migration in anisotropic media. With this new method, the demands on traveltimes engines can be significantly reduced by avoiding dynamic ray tracing: the application of dynamic ray tracing requires continuous first- and second-order spatial derivatives of the elastic parameters. Furthermore, ray methods can fail in the vicinity of shear wave singularities. Therefore, alternative traveltimes algorithms are better suited for anisotropic media than dynamic ray tracing. However, most of these implementations do not allow the computation of dynamic wavefield properties, which are required for the true-amplitude weight functions. With the new method, only traveltimes are used as input for the computation of the weights. Our examples demonstrate that the method allows the reconstruction of the structures as well as the amplitudes with high fidelity.



(a)



(b)

Figure 2: (a) The depth-migrated PP section, and (b) the depth-migrated PS section. Due to the asymmetry of the ray paths, the considered offset range is different for the PP and the PS case.

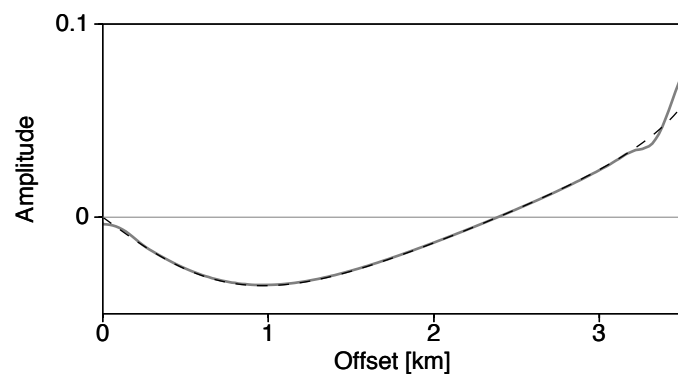
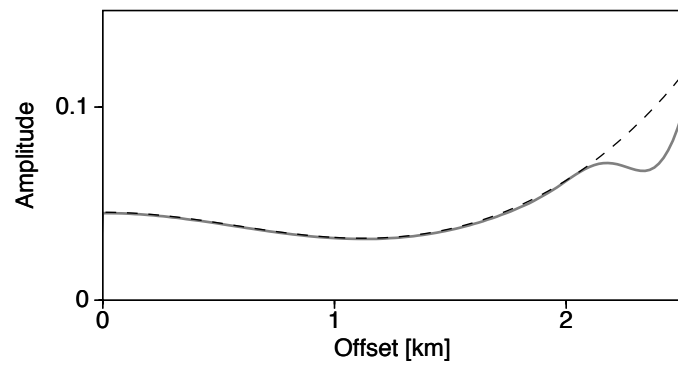


Figure 3: AVO for (a) PP reflections and (b) PS reflections: the reconstructed reflectivities (solid grey lines) coincide with the analytic solution (dashed black lines). Due to the asymmetry of the ray paths, the displayed offset range is different for the PP and the PS case.

ACKNOWLEDGEMENTS

We thank the members of the Applied Seismics Group in Hamburg for continuous discussion. This work was partially supported by the German Research Foundation (DFG; grants Va 207/1-3) and the sponsors of the Wave Inversion Technology (WIT) consortium.

REFERENCES

- Bleistein, N. (1984). *Mathematical methods for wave phenomena*. Academic Press.
- Bleistein, N. (1986). Two-and-one-half dimensional in-plane wave propagation. *Geophysical Prospecting*, 34:686–703.
- Červený, V. (2001). *Seismic Ray Theory*. Cambridge University Press.
- Červený, V. and Pšenčík, I. (1972). Rays and travel-time curves in inhomogeneous anisotropic media. *Journal of Geophysics*, 38:565–577.
- Coman, R. and Gajewski, D. (2005). Traveltime computation by wavefront-oriented ray tracing. *Geophysical Prospecting*, 53:23–36.
- Daley, P. F. and Hron, F. (1979). Reflection and transmission coefficients for seismic waves in ellipsoidally anisotropic media. *Geophysics*, 44:27–38.
- de Hoop, M. and Bleistein, N. (1997). Generalized Radon transform inversions for reflectivity in anisotropic elastic media. *Inverse Problems*, 13:669–690.
- de Hoop, M., Spencer, C., and Burridge, R. (1999). The resolving power of seismic amplitude data: an anisotropic inversion/migration approach. *Geophysics*, 64:852–873.
- Dillon, P., Ahmed, H., and Roberts, T. (1988). Migration of mixed-mode VSP wavefields. *Geophysical Prospecting*, 36:825–846.
- Druzhinin, A. (2003). Decoupled elastic prestack depth migration. *Journal of Applied Geophysics*, 54:369–389.
- Ettrich, N. and Gajewski, D. (1998). Traveltime computation by perturbation with FD-eikonal solvers in isotropic and weakly anisotropic media. *Geophysics*, 63:1066–1078.
- Ettrich, N., Gajewski, D., and Kashtan, B. M. (2001). Reference ellipsoids for anisotropic media. *Geophysical Prospecting*, 49:321–334.
- Gajewski, D. (1993). Radiation from point sources in general anisotropic media. *Geophysical Journal International*, 113:299–317.
- Gerea, C., Nicoletis, L., and Granger, P.-Y. (2000). Multi component true amplitude anisotropic imaging. In *Expanded Abstracts*. Soc. Expl. Geophys.
- Juhlin, C. and Windhofer, M. (1992). Anisotropy and mis-ties in seismic data: A modelling study. *Exploration Geophysics*, 23:167–172.
- Kaschwich, T. and Gajewski, D. (2003). Wavefront-oriented ray tracing in 3D anisotropic media. In *Expanded Abstracts*. EAGE.
- Martins, J. L., Schleicher, J., Tygel, M., and Santos, L. (1997). 2.5-D true-amplitude migration and demigration. *Journal of Seismic Exploration*, 6:159–180.
- Pšenčík, I. and Teles, T. N. (1996). Point source radiation in inhomogeneous anisotropic structures. *Pure and Applied Geophysics*, 148:591–623.

- Schleicher, J., Tygel, M., and Hubral, P. (1993). 3D true-amplitude finite-offset migration. *Geophysics*, 58:1112–1126.
- Schleicher, J., Tygel, M., Ursin, B., and Bleistein, N. (2001). The Kirchhoff-Helmholtz integral for anisotropic elastic media. *Wave Motion*, pages 353–364.
- Sena, A. and Toksöz, M. N. (1993). Kirchhoff migration and velocity analysis for converted and nonconverted waves in anisotropic media. *Geophysics*, 58:265–276.
- Soukina, S., Gajewski, D., and Kashtan, B. (2003). Traveltime computation for 3-D anisotropic media by a finite-difference perturbation method. *Geophysical Prospecting*, 51:431–441.
- Thomsen, L. (2002). *Understanding Seismic Anisotropy in Exploration and Exploitation*. Distinguished Instructor Series, No. 5, SEG, Tulsa.
- Tsvankin, I., Gaiser, J., Grechka, V., van der Baan, M., and Thomsen, L. (2012). Seismic anisotropy in exploration and reservoir characterization. *Geophysics*, 75:75A15–75A29.
- Vanelle, C. and Gajewski, D. (2002). Second-order interpolation of traveltimes. *Geophysical Prospecting*, 50:73–83.
- Vanelle, C. and Gajewski, D. (2003). Determination of geometrical spreading from traveltimes. *Journal of Applied Geophysics*, 54:391–400.
- Vanelle, C. and Gajewski, D. (2009). Application of Snell's law in weakly anisotropic media. *Geophysics*, 74:WB147–WB152.
- Vanelle, C., Spinner, M., Hertweck, T., Jäger, C., and Gajewski, D. (2006). Traveltime-based true-amplitude migration. *Geophysics*, 71:S251–259.